ATP signaling is deficient in cultured Pannexin1-null mouse astrocytes

Sylvia O. Suadicani[*,+], **Rodolfo Iglesias**[*], **Junjie Wang**[#], **Gerhard Dahl**[#], **David C. Spray**[*], and **Eliana Scemes**[*]

[*]Dominick P. Purpura Department of Neuroscience, Albert Einstein College of Medicine, Bronx, NY, 10461, USA

[+]Department of Urology, Albert Einstein College of Medicine, Bronx, NY, 10461, USA

[#]Department of Physiology and Biophysics, University of Miami, School of Medicine, PO Box 016430, Miami, FL, 33101, USA

Abstract

Pannexins (Panx1, 2 and 3) comprise a group of proteins expressed in vertebrates that share weak yet significant sequence homology with the invertebrate gap junction proteins, the innexins. In contrast to the other vertebrate gap junction protein family (connexin), pannexins do not form intercellular channels, but at least Panx1 forms non-junctional plasma membrane channels. Panx1 is ubiquitously expressed and has been shown to form large conductance (500pS) channels that are voltage-dependent, mechanosensitive and permeable to relatively large molecules, such as ATP. Pharmacological and knockdown approaches have indicated that Panx1 is the molecular substrate for the so-called "hemichannel" originally attributed to connexin43 (Cx43) and that Panx1 is the pore forming unit of the $P2X_7$ receptor. Here, we describe, for the first time, conductance and permeability properties of Panx1-null astrocytes. The electrophysiological and fluorescence imaging analysis performed on these cells fully support our previous pharmacological and Panx1 knockdown studies that showed profoundly lower dye uptake and ATP release than wild-type untreated astrocytes. As a consequence of decreased ATP paracrine signaling, intercellular calcium wave spread is altered in Panx1-null astrocytes. Moreover, we found that in astrocytes as in Panx1 expressing oocytes, elevated extracellular K^+ activates Panx1 channels independently of membrane potential. Thus, based on the present findings and our previous report, we propose that Panx1 channels serve as K^+ sensors for changes in the extracellular milieu such as those occurring under pathological conditions.

Keywords

Gap junction; P2X receptor; calcium waves; glia; connexin; pannexin

INTRODUCTION

There is controversy in the literature regarding the non-vesicular pathways by which ATP is released from astrocytes and other cell types and through which dye molecules can be taken up. The two main candidates for such roles are currently "hemichannels" formed by the gap

Correspondence to: Eliana Scemes, Dominick P. Purpura Department of Neuroscience, Albert Einstein College of Medicine, 1410, Pelham Parkway, Kennedy Center, room 203, Bronx, NY, 10461, Phone: (001) (718) 430-3303, eliana.scemes@einstein.yu.edu.

junction connexin proteins [where the principal candidate in most cell types is connexin43 (Cx43)] and non-junctional channels formed by pannexin1 (Panx1).

Connexins are the pore forming elements of vertebrate gap junction channels, while invertebrate gap junctions use totally unrelated (but topologically similar) proteins termed innexins. Pannexins comprise a group of proteins with weak yet significant homology to innexins that was discovered 10 years ago through homology searches of mammalian sequence databases (Baranova et al. 2004; Panchin et al. 2000, 2005). Despite initial studies suggesting that pannexins might form gap junction channels (Bruzzone et al. 2003), it is now widely accepted that pannexins, at least Panx1, form plasma membrane channels and do not function as intercellular channels [reviewed in (Dahl and Locovei 2006; Scemes 2011; Sosinsky et al. 2011)].

Gap junction "hemichannels" formed of Cx43 have been implicated in ATP release and/or dye uptake in a variety of cell types under various conditions. The identity of the channel was inferred from the inhibition of dye uptake and ATP release by certain gap junction channel blockers (Contreras et al. 2002; De Vuyst et al. 2007; Kang et al. 2008) and connexin-mimetic peptides (Clarke et al. 2009; Leybaert et al. 2003) and reported absence in Cx43-null astrocytes (Contreras et al. 2003; Retamal et al. 2007). However, Panx1 channels are even more sensitive to most gap junction channel blockers (Bruzzone et al. 2005) including connexin-mimetic peptides (Dahl 2007) than are channels formed of connexins. Panx1 channels are opened by activation of the $P2X_7$ receptor (Locovei et al. 2007; Pelegrin and Surprenant 2006), membrane stretch (Bao et al. 2004) and high extracellular K^+ concentration (Silverman et al. 2009), all of which can occur under physiological and pathological conditions, and both ATP release and dye uptake induced by these stimuli are blocked by Panx1 knockdown strategies (Iglesias et al. 2008, 2009a,b).

Missing, however, has been a mouse model in which Panx1 is deleted, so that its role in physiology as well as cell properties could be inferred from functions absent in the knockout. Several mouse lines are newly available in which Panx1 has been deleted using different strategies, and we have recently shown in two of the mouse models that we have tested, the severity of kainic acid-induced seizures was markedly and consistently reduced (Santiago et al. 2011). We now provide data indicating that ATP release and other phenomena that have been associated with Cx43 hemichannels or to the P2Z pore are absent in astrocytes from these mice.

MATERIAL and METHODS

Panx1-null mice

Heterozygous (HT) Panx1$^{tm1a(KOMP)Wtsi}$ mice were purchased from the Knockout Mouse Project (KOMP) at UCDavis and maintained in IACUC approved animal facilities at Albert Einstein College of Medicine. Mice homozygous for the transgene (Panx1$^{-/-}$) and wild-type (Panx1$^{+/+}$) littermates were obtained by breeding HT mice. Tail PCR was performed on progeny using the specific primers, as previously described (Santiago et al., 2011). All studies used protocols approved by the Einstein Animal Care and Use Committee.

Astrocyte cultures

Brain cortices of neonatal (P0) Panx1$^{+/+}$ and Panx1$^{-/-}$ mice were minced in ice cold Ca^{2+}-free Dulbecco's phosphate buffered saline (DPBS, Cellgro, Herndon, VA, USA) and tissue digested with 0.05% trypsin (Cellgro) for 5 min at 37°C, after which digests were centrifuged at 1.500 RPM for 5 min. Supernatants were removed and cells re-suspended in Dulbecco's minimal essential medium (DMEM, Invitrogen, NY, USA) containing 10% fetal bovine serum (FBS, Invitrogen) and 1% penicillin/streptomycin antibiotics (Invitrogen).

Cells were grown for 1–2 weeks in plastic tissue cultures dishes (BD Falcon, NJ, USA) and maintained at 37°C in a humidified 5% CO_2 incubator.

Electrophysiology

Solitary Panx1$^{+/+}$ and Panx1$^{-/-}$ astrocytes were plated on glass coverslips 6 hrs prior to recordings. Whole cell patch clamp recordings were performed on cells that were round and exhibited no or few short processes, as previously described (Iglesias et al., 2009). Briefly, cells were bathed in external solution containing (mM): NaCl 147, Hepes 10, glucose 13, $CaCl_2$ 2, $MgCl_2$ 1 and KCl 5, pH 7.4; K^+ was varied through equimolar substitution of KCl with NaCl. The pipette solution contained (mM): CsCl 130, EGTA 10, Hepes 10, $CaCl_2$ 0.5. Activation of Panx1 channels by voltage was performed using a 5.5 second voltage ramp protocol from a holding potential of −60mV to +80mV. To analyze the participation of Panx1 channels in agonist-induced $P2X_7R$ activation, astrocyte membrane potential was held at −60mV and the $P2X_7R$ agonist BzATP (50 or 100μM; Sigma-Aldrich, MO, USA) was superfused for 5–10 seconds. After the first response to the agonist, the gap junction channel blockers carbenoxolone (50μM; CBX; Sigma-Aldrich) and mefloquine (100nM; MFQ; QU-024 Bioblocks, CA, USA) were superfused for 5 min prior to the addition of the P2R agonist. Electrophysiological recordings were accomplished using an Axopatch 200B amplifier and pClamp9 software was used for data acquisition and analysis.

Oocytes

Oocytes were prepared as described previously (Dahl et al. 1992). *Xenopus laevis* oocytes were isolated by incubating small pieces of ovary in 2 mg ml^{-1} collagenase in calcium free oocyte Ringer's solution (OR2) and stirring at 1 turn/second for three hours at room temperature. After being thoroughly washed with regular OR2, oocytes devoid of follicle cells and having uniform pigmentation were selected and stored in OR2 at 18°C. OR2 solution in mM: 82.5 NaCl, 2.5 KCl, 1.0 $MgCl_2$, 1.0 $CaCl_2$, 1.0 Na_2HPO_4, 5.0 HEPES, antibiotics (Penicillin, 10,000 units/ml; Streptomycin, 10 mg/ml, pH7.5).

In vitro transcription of mRNAs—The vector pCS2 containing mouse Panx1 cDNA was linearized with Not1. mRNA was transcribed by Sp6 RNA Polymerase from 10 μg of linearized plasmid using the mMessage mMachine kit (Ambion). mRNA was quantified by absorbance (260nm), and the proportion of full-length transcripts was checked by agarose gel electrophoresis. 20 nl of mRNA (50 ng/μl) was injected into oocytes. The injected oocytes were then incubated at 18°C for 18–24 hours.

Voltage clamp—Whole cell voltage clamp recording was performed with two intracellular electrodes as described (Dahl et al., 1992) using a Gene Clamp 500B apparatus (Axon Instruments). Voltage ramps of 70 second duration were applied with a custom made device.

Dye uptake

Astrocytes (Panx1$^{+/+}$ and Panx1$^{-/-}$) plated on glass bottomed dishes (MatTek, MA, USA) were bathed for 5 min in phosphate buffered solution (PBS, pH 7.4) containing the cell-impermeant dye YoPro-1 (5 μM; Molecular Probes-Invitrogen). Cells were then exposed to a solution containing 300 μM BzATP and 5 μM of the dye or to 10 mM K^+ solution containing 5 μM YoPro1. YoPro1 fluorescence intensity was measured during 500 sec BzATP and high K^+ solution stimulation, as previously described (Iglesias et al., 2009a). YoPro1 fluorescence was captured with Metafluor software Molecular Devices, CA, USA) using a CoolSNAP-HQ2 CCD camera (Photometrics, AZ, USA) attached to an inverted Nikon microscope (Eclipse TE-2000E, Nikon, Japan) equipped with a 20X dry objective and FITC filter set.

ATP release

Confluent cultures of Panx1$^{+/+}$ and Panx1$^{-/-}$ astrocytes plated in 35 mm dishes were washed twice in PBS and then exposed for 3 min to PBS containing 300μM BzATP. After complete removal and washout of the agonist, cells were bathed in PBS for 2 min before collection of samples of BzATP-induced ATP release. For measurements of ATP released following exposure to high K$^+$ solution, cells were exposed to 10mM K$^+$ solution for 2 min before collection of samples. The amount of ATP in samples was measured as previously described (Iglesias et al., 2009), using the luciferin/luciferase assay (Molecular Probes-Invitrogen) and a plate reader luminometer (Veritas, Turner Instruments, CA, USA). The amount of ATP in each sample was calculated from standard curves and normalized for the protein concentration, using the BCA assay (Pierce, Rockford, IL, USA).

Intercellular calcium waves

Astrocytes plated on glass bottomed (MatTek) dishes were loaded with Fluo-3 AM (7 μM; Molecular Probes-Invitrogen) for 45 min at 37°C. After several washes with DPBS (pH 7.4), cells were imaged on a Nikon TE2000 inverted microscope equipped with a CCD digital camera (Orca-ER; Hamamatsu Photonics, Hamamatsu, Japan) and a 10× panfluo objective (numerical aperture, 0.45; Nikon). Changes in Fluo-3 fluorescence intensities emitted at excitation 480 nm wavelength were acquired at one Hz using the Lambda DG-4 (Sutter Instruments, Novato, CA) driven by a computer through Metafluor software. Intercellular calcium waves (ICWs) were triggered by focal mechanical stimulation of single cells in the center of the microscope field of view (460 × 367 μm), as described previously (Suadicani et al. 2006). ICWs were analyzed in terms of the extent of spread.

Dye coupling

The scrape loading (el-Fouly et al. 1987) and micro-injection techniques were used to evaluate the degree of gap junctional communication, as previously described (De Pina-Benabou et al. 2001; Thi et al. 2010). For the scrape loading, Panx1$^{+/+}$ and Panx1$^{-/-}$ astrocytes plated in 35 mm dishes to confluency were bathed in DPBS, pH 7.4, containing 0.5 mg/mL Lucifer yellow (LY; Sigma-Aldrich). Using a razor blade, two scrapes per dish allowed the dye to enter the damaged cells. Five minutes after scraping, preparations were washed five to six times with DPBS and then fixed in 4% *p*-formaldehyde (Electron Microscopy Sciences, PA, USA) and photographed using Metafluor software and a CoolSNAP-HQ2 CCD camera attached to an inverted Nikon microscope (Eclipse TE-2000E) equipped with a 10X dry objective and FITC filter set. To determine the extent of LY spread from the scrape edge to adjacent cells, the optical density profile of LY obtained using Scion NIH Image software was used. Values of LY spread were obtained by averaging the maximal distances at which LY fluorescence could be detected; at least four measurements of LY spread were obtained along each single scrape line in three independent experiments. Fractional changes in LY spread were calculated as [($d_{test}/d_{control}$) − 1]. For LY microinjections, single astrocytes in confluent cultures were impaled with a glass microelectrode containing LY (5% weight in 150 mM LiCl). LY iontophoresis was performed by applying 0.1 μA current for 3 min using an electrometer (Model 3100; A-M Systems Inc, WA, USA). LY fluorescence images were acquired immediately after removal of the microelectrode from the injected cells. Quantification of the degree of dye coupling was performed by measuring the distance of LY spread from the injected cells. At least 18 microinjections were performed in 3–5 independent experiments.

Western blot

Samples of whole cell lysates of Panx1$^{+/+}$ and Panx1$^{-/-}$ astrocytes were electrophoresed in 4–20% SDS-PAGE (Bio-Rad, Hercules, CA) and then transferred to nitrocellulose

membranes (Schleicher & Schuell, Keene, NH, USA). Immunoblots were performed after overnight incubation of membranes with blocking solution consisting of 1X PBS containing 2% dry nonfat milk and 0.4% polyoxyethylenesorbitan monolaurate (Tween-20; Sigma) using primary antibodies. After several washes with 1X PBS-Tween-20, membranes were incubated with HRP-conjugated secondary antibodies (1:2000; Santa Cruz Biotechnology, Santa Cruz, CA, USA). Detection of bands was performed on X-ray films (Kodak, Rochester, NY, USA) following incubation with enhanced chemiluminescence reagents (Amersham Pharmacia Biotechnology, Piscataway, NJ, USA). Quantification of the expression levels of Cx43 and Panx1 was performed by densitometric analysis (Scion-NIH Image software) using GAPDH as an invariant control against which the protein of interest was normalized. The following primary antibodies were employed: polyclonal anti-Panx1 (1:1000; Aves Labs), polyclonal anti-Cx43 (1:5000; Sigma), polyclonal anti-$P2X_7$ receptor (1:500; Alomone), and monoclonal anti-GAPDH antibodies (1:5000; Fitzgerald).

Statistical Analysis

Data were expressed as mean ± s.e.m. ANOVA analysis of variance followed by Tukey's multiple comparison tests was performed when three or more groups were compared. Student's t-test was used when two groups were analyzed.

RESULTS

Electrophysiological features of Pannexin1 currents: activation by voltage, elevated extracellular K^+ and following $P2X_7$ receptor stimulation

Pannexin1 channels expressed in *Xenopus* oocytes have been shown to be activated by elevated extracellular K^+ even when held at potentials at which the channels are normally closed (Silverman et al., 2009). When bathed in 2.5 mM K^+ concentration Ringer solution, Panx1 currents were activated at potentials close to -5 mV when voltage ramps (−100 to +100mV) were applied (Figure1A). Five min incubation of oocytes in 50 mM K^+ solution shifted the activation voltage of Panx1 channels and significantly increased current amplitudes (Figure 1A). In response to the elevated K^+ concentration the channels were already open while held at −100 mV and stayed open throughout the voltage ramp to +100 mV. As compared to the same oocyte exposed to regular K^+ concentration (2.5 mM), the reversal potential was shifted to the left. Similar results were obtained by exposure of the cells to 10 mM K^+ (not shown), except that the current amplitudes were lower, as would be expected from a dose-dependent process. Dose dependency is shown in Figures 1B and C. Compared to Panx1 currents evoked by +10 mV voltage steps (from a holding potential of −60 mV to −50mV) in oocytes bathed in 2.5 mM K^+ solution, significant increases in current amplitudes were recorded when cells were bathed in 10, 20, and 50 mM K^+ and similar voltage steps applied (Figure 1C).

In astrocytes, Pannexin1 currents are also evident from electrophysiological recordings in response to voltage ramps (holding potential of −60mV; ramps from −60mV to +80 mV, at 28 mV/sec) as nonlinearities above 0 mV (Figure 2A). In Panx1$^{−/−}$astrocytes bathed in 5 mM K^+ solution, such outward currents are smaller compared to Panx1$^{+/+}$ cells (Figure 2A); in this condition, current amplitudes, as measured by the ratio between non-linear to linear currents (current amplitudes at +80 mV divided by current amplitudes at −60 mV), were significantly reduced in Panx1$^{−/−}$ compared to Panx1$^{+/+}$ (Panx1$^{+/+}$ ratio: 5.29 ± 1.28, N= 13 cells; Panx1$^{−/−}$ ratio: 2.14 ± 0.58, N=16 cells; P=0.024, unpaired t-test). However, when bathed in 2 mM K^+ no statistically significant difference in the ratio of non-linear to linear currents was detected in experiments with Panx1$^{+/+}$ and Panx1$^{−/−}$ astrocytes (Panx1$^{+/+}$ ratio: 4.39 ± 0.74, N = 8 cells; Panx1$^{−/−}$ ratio: 3.02 ± 0.13, N = 10 cells; P = 0.059, unpaired t-test). Thus, these results besides indicating that Panx1 channels are activated by membrane

depolarization, suggest that opening of Panx1 channels is modulated by extracellular K^+ concentration.

To further evaluate the extent to which native Panx1 channels are activated by elevated extracellular K^+, we used cultured astrocytes from Panx1$^{+/+}$ and Panx1$^{-/-}$ mice. Whole cell recordings of solitary Panx1$^{+/+}$ astrocytes exposed to elevated extracellular K^+ indicated that the activation voltage of Panx1 channels was shifted to more negative potentials when extracellular K^+ was raised from 4 to 12 mM (Figure 2B). The shift in the activation voltage was reversed by exposing the cells to lower 2.5 mM K^+ solutions (Figure 2B). When bathed in 10 mM K^+ solution, Panx1 currents measured at +60 mV were increased 1.5 fold compared to those recorded from cells exposed to 2.5 mM K^+ (Figures 2C–D). In contrast, Panx1$^{-/-}$ astrocytes did not display such K^+-sensitive currents (Figures 2C–D). It should be noted that conductance of 9 out of 10 Panx1$^{+/+}$ astrocytes increased as K^+ was elevated while conductance of every Panx1$^{-/-}$ astrocyte was decreased or unchanged (Figure 2C). Thus, similarly to mPanx1 channels expressed in oocytes, opening of native Panx1 channels in astrocytes occurs at elevated extracellular K^+ independently of membrane potential.

We have previously shown that in response to brief exposure to 50 μM BzATP, Panx1$^{+/+}$ astrocytes rapidly respond with two current components, a small amplitude current that is followed by large amplitude current (Iglesias et al., 2009a); this second component is sensitive to mefloquine (MFQ, a Panx1 inhibitor: Iglesias et al., 2009b), resulting in BzATP-induced currents of reduced amplitudes (Figure 3A). In contrast, Panx1$^{-/-}$ astrocytes respond to prolonged application of 100 μM BzATP with only low amplitude, MFQ-insensitive currents (Figure 3B; Iglesias et al., 2009b), supporting the idea that Panx1 channels are responsible for the second current component activated following P2X$_7$ receptor stimulation. Figure 3C shows the bar histograms of the mean amplitude values of BzATP-induced currents [for each bar, means ± s.e.m. are from 4–6 recordings]. In Panx1$^{+/+}$ astrocytes, BzATP-induced currents (352.5 ± 30 pA) were significantly reduced (P<0.01) in the presence of mefloquine (MFQ 100 nM; 105 ± 18 pA), or carbenoxolone (CBX 50 μM; 90 ± 27 pA), and were also low in untreated Panx1$^{-/-}$ astrocytes (101 ± 16 pA).

Western blot analysis of astrocyte cultures derived 6 Panx1$^{+/+}$ and 6 Panx1$^{-/-}$mice indicated no changes in P2X$_7$ receptor expression levels between the two genotypes (Figure 4), indicating that reduced P2X$_7$ currents in Panx1$^{-/-}$ cells are not related to decreased expression of these receptors but rather to the lack of Panx1 expression.

Permeability features of Panx1$^{-/-}$ astrocytes

Following 500 sec BzATP (300 μM) stimulation, a significant increase in YoPro-1 fluorescence was recorded from Panx1$^{+/+}$ astrocytes compared to non-stimulated Panx1$^{+/+}$ cells (Figure 5A). Under this condition, there was a 1.34 ± 0.1 fold increase in dye uptake (N = 300 cells from 3 independent experiments). This increase in dye uptake was much lower when BzATP was bath applied to Panx1$^{-/-}$ astrocytes (Figure 5A). In this case, only a 1.04 ± 0.01 fold increase in YoPro fluorescence (N = 800 cells from 8 independent experiments) was measured.

Under similar conditions, BzATP-induced ATP release seen in Panx1$^{+/+}$ astrocytes was totally absent in Panx1$^{-/-}$ astrocytes (Figure 5B). After BzATP stimulation of Panx1$^{+/+}$ astrocytes, there was a 3.12 ± 0.13 fold increase in extracellular ATP compared to that recorded from non-stimulated Panx1$^{+/+}$ cells (Figure 5B). For Panx1$^{-/-}$astrocytes, the extracellular levels of this purine induced by the same stimulation were significantly (P<0.001) lower when compared to non-stimulated Panx1$^{-/-}$ cells (Figure 5B).

Similar results to those described above were obtained when astrocytes were exposed to 10 mM K^+ solution. After high K^+ stimulation, there was 1.24 ± 0.03 fold increase in YoPro uptake compared to that measured from non-stimulated Panx1$^{+/+}$ cells (Figure 5C). In contrast to Panx1$^{+/+}$ astrocytes, high K^+ solution bath applied to Panx1$^{-/-}$ cells evoked a small (0.96 ± 0.001 fold) but significant decrease in YoPro-1 fluorescence compared to non-stimulated Panx1$^{-/-}$ cells (P<0.001; Figure 5C).

The 2.64 ± 0.13 fold increase in extracellular ATP measured following high K^+ stimulation of Panx1$^{+/+}$ astrocytes (Figure 5D) was altogether absent in Panx1$^{-/-}$ cells (Figure 5D).

Absence of calcium wave amplification in Panx1$^{-/-}$ astrocytes

Gap junctional communication and extracellular ATP-mediated P2 receptor stimulation are the two pathways involved in the transmission of calcium waves between astrocytes [reviewed in (Scemes and Giaume 2006)]. Increased distance of transmission of calcium waves between cultured astrocytes has been proposed to involve a mechanism of ATP-induced ATP release (Anderson et al. 2004) which we have shown to involve the ATP sensitive P2X$_7$ receptor and the ATP-releasing channel Panx1 (Suadicani et al. 2006; Suadicani et al. 2009).

Focal mechanical stimulation of single Panx1$^{+/+}$ astrocytes in confluent cultures bathed in DPBS led to a calcium waves that spread to a distance of 186.9 ± 7.84 μm (N = 53) from the point of stimulation (Figure 6). When bathed in low divalent cation concentration solution (LDPBS: nominal zero Ca^{2+} and 43 μM $MgCl_2$), the distance of calcium wave transmission significantly increased (P<0.001), spreading to 274.2 ± 9.5 μm (N = 44) from the point of stimulation (Figure 6A). This 1.5 fold increase in the transmission distance of calcium waves was totally abrogated in Panx1$^{-/-}$ astrocytes (Figure 6B). When bathed in PBS, the radius of calcium wave transmission between Panx1$^{-/-}$ astrocytes was 279.4 ± 9.1 μm (N = 48), which was not significantly different from that measured in Panx1$^{-/-}$ cells bathed in LDPBS (Figures 6A, B; 266.4 ± 10.0 μm; N=36; P>0.05). Interestingly, the radius of calcium waves traveling between Panx1$^{-/-}$ astrocytes bathed in PBS was significantly higher than that measured from Panx1$^{+/+}$ cells (Figure 6A; P<0.001). This appears to be due to altered gap junctional communication as described below.

Increased coupling and connexin43 expression in Panx1$^{-/-}$ astrocytes

To evaluate whether the larger extent of calcium wave spread recorded in Panx1$^{-/-}$ astrocytes bathed in PBS compared to that of Panx1$^{+/+}$ was related to coupling strength, we compared gap junctional coupling between these cells using the scrape loading and dye-injection techniques. As shown in Figures 7A-B, Panx1$^{-/-}$ astrocytes are better coupled than Panx1$^{+/+}$ cells. Analyses of LY microinjections indicated a significant increase in dye coupling in Panx1$^{-/-}$ cells (125.5 ± 3.7 μm; N = 18 injections from 5 independent experiments) compared to Panx1$^{+/+}$ astrocytes (78.4 ± 2.0 μm; N = 26 injections from 3 independent experiments) (Figure 7A). Similarly, the scrape loading technique revealed a 2 fold increase in LY spread, from 107.3 ± 8.3 μm (N = 28 measurements from 6 independent experiments) in Panx1$^{+/+}$ astrocyte cultures to 213.4 ± 9.1 μm (N = 29 measurements from 7 independent experiments) in Panx1$^{-/-}$ cultures (Figure 6B; P<0.001).

This increased dye coupling recorded in Panx1$^{-/-}$ astrocytes is likely to be due to the 1.6 fold increase in Cx43 expression levels measured in western blots of these cells compared to that measured in Panx1$^{+/+}$ cells. (Figure 7C; P = 0.02; N = 4).

DISCUSSION

Pannexins comprise a group of proteins that bear no sequence homology to connexins but have been included in the gap junction family due to their sequence homology with the invertebrate gap junction proteins, the innexins (Panchin et al. 2000). Pannexin1 (Panx1) is the best characterized of the three pannexins present in the rodent and human genomes. Panx1 is widely distributed in mammalian tissues and forms plasma membrane channels with large conductance (~500 pS) that are permeable to ATP (Bao et al. 2004; Locovei et al. 2006a). Although Panx1 does not share sequence homology with connexins, several compounds known to block gap junction channels are effective in blocking Panx1 channels, even at much lower concentrations (Bruzzone et al. 2005; Iglesias et al. 2009b). Such overlap in pharmacology is not surprising as most gap junction channel blockers were first identified in invertebrate preparations, but it imposes some difficulties when evaluating the contribution of connexins and pannexins to biological processes. Recently, Panx1 knockout mouse lines were generated by three independent groups (Dr. H. Monyer, Genentech and by Knockout Mouse Project -KOMP) and reports on these mice in general support the role of Panx1 as an ATP releasing channel (Qiu et al. 2011; Qu et al. 2011; Santiago et al. 2011; Seminario-Vidal et al. 2011). Interestingly, however, Panx1 and Panx2 double knockout mice were reported not to show the phenotype of depressed ATP release seen in the single Panx1 knockout mice (Bargiotas et al., 2011). Although we do not know the reason for such divergency, it is possible that genetic differences may have accounted for this discrepancy.

We have previously shown that Panx1 channels in cultured neurons and astrocytes can be activated by elevated extracellular K^+ concentrations (Silverman et al. 2009). Similarly, in hippocampal slices, rise in extracellular K^+ as occurs under intense neuronal activity (epileptiform activity) was recently shown to lead to the influx of the dye YoPro-1 and to the release of ATP in a Panx1 dependent manner (Santiago et al. 2011). The mechanism by which K^+ activates Panx1 channels is likely to involve direct interaction of the cation with the channel, which is shown here to induce a shift toward lower activation voltage when extracellular K^+ rises. That the action of K^+ is direct is also supported by the fact that in *Xenopus* oocytes expressing mPanx1 channels similar effects on the activation voltage was recorded. Nevertheless, it is possible that under non-voltage clamp conditions, intracellular signaling pathways may also modulate Panx1 channels when extracellular K^+ concentration increases. Such a mechanism may be synergistic with the facilitation of Panx1 opening due to the depolarization induced by K^+. Among the possible mechanisms, intracellular calcium elevation due to the influx of calcium through L-type calcium channels (De Pina-Benabou et al. 2001) has been shown to induce opening of Panx1 channels either directly or as a consequence of purinergic receptor activation (Locovei et al. 2006b). In the presence of 10 mM K^+, increased outward currents, YoPro1 uptake and ATP release from cultured astrocytes were totally eliminated in astrocytes lacking Panx1. Thus, Panx1 channels may be regarded as having a dual function as sensors and as "paracrine" channels.

Here we show for the first time using the KOMP transgenic mice lacking Panx1 that in cultured astrocytes channels formed by this protein are the main pathway for ATP release following $P2X_7$ receptor stimulation, which we have shown to contribute to the amplification of calcium waves (Scemes et al. 2007; Suadicani et al. 2006). These new findings, besides supporting our previous studies indicating the involvement of Panx1 in purinergic transmission between astrocytes (Iglesias et al. 2009a; Scemes et al. 2007), clearly show that Panx1 channels in astrocytes are the major ATP permeation pathway induced by $P2X_7$ receptor stimulation. The original studies indicating that the permeabilization "pore" of the $P2X_7$ receptor was the Panx1 channel (Locovei et al. 2007; Pelegrin and Surprenant 2006) have been debated based on knockdown and pharmacological assays and reports suggesting that $P2X_7$ receptor activation triggers distinct

"permeabilization" pathways for cations and anions (Pelegrin and Surprenant 2007, 2009; Schachter et al. 2008). Data presented here clearly indicate that in astrocytes Panx1 is the main permeation pathway for the flux of both positively and negatively charged molecules such as YoPro1 and ATP following activation of P2X$_7$ receptors. Nevertheless, we cannot rule out that a Panx1-independent pathway may also provide for the flux of charged molecules, as reported in macrophages (Marques-da-Silva et al. 2011). However, given that Panx1 channel currents reversed close to zero mV under symmetrical KCl or K$^+$-gluconate conditions (Bao et al. 2004), it is expected that both cationic and anionic dyes or molecules would equally permeate these channels.

In astrocytes, the release of "gliotransmitters" such as ATP has been proposed to occur via both vesicular and non-vesicular pathways [reviewed in (Hamilton and Attwell 2010; Parpura et al. 2004)], and in astrocytes both Cx43 hemichannels and Panx1 channels have been proposed as non-vesicular routes (Iglesias et al. 2009a; Kang et al. 2008; Ye et al. 2003). The present results showing complete absence of ATP release from Panx1-null astrocytes following elevated extracellular K$^+$ stimulation or following P2X$_7$ receptor activation are in favor of the idea that Panx1 channels represent the main pathway for ATP release from these cells. Nevertheless, we cannot exclude that other mechanisms may also contribute to this release when stimuli other than the ones investigated in the present study are in play. For instance, in case of connexin43 mutations, such as that associated with oculodentodigital dysplasia, hypoxia and low [Ca^{2+}]$_o$ were reported to lead to increased ATP release due to enhanced opening of the mutated Cx43^{G138R} hemichannels (Dobrowosky et al., 2008; Torres et al., 2012).

Paracrine signaling and gap junctional communication are the two pathways by which astrocytes communicate via calcium waves [reviewed in (Scemes and Giaume, 2006)]. This form of communication is highly plastic, such that when one of these two pathways is altered ICWs can be preserved by a compensatory mechanism. As we originally proposed based on purinergic signaling alteration in Cx43-null astrocytes (Scemes et al., 2000; Suadicani et al., 2003), our present results showing up-regulation of Cx43 in Panx1-null astrocytes, indicate that in the absence of the ATP releasing channel, increased gap junctional communication may sustain the transmission of ICW in Panx1-null cells. Similarly, increased contribution of purinergic signaling in the transmission of calcium waves when gap junctional communication was decreased was previously reported for astrocytes treated with IL1-β (John et al. 1999). These studies thus indicate that gap junction proteins (connexins and pannexins) and purinergic receptors form a calcium signaling unit in which components can be reciprocally regulated (Iacobas et al. 2008). The recent report showing absence of calcium wave spread in astrocytes of Cx30/Cx43 double knockout mice (Torres et al., 2012) is consistent with this because gap junctional communication was abolished along with putative Cx43 hemichannel function.

As mentioned above, pannexins are unlikely to form gap junction channels between native cells. Nevertheless, it has been claimed that Panx1 can form gap junction channels under conditions of massive over-expression (Bruzzone et al. 2003; Lai et al. 2007). However, canonical gap junction structures formed by Panx1 have not been observed by electron microscopy in either transfected cells or in native tissues and nor have gap junction channels induced by Panx1 overexpression in mammalian cells been characterized [see (Sosinsky et al. 2011)]. The present study showing that Cx43 expression and gap junction coupling are substantially higher in Panx1-null than in wild-type astrocytes support the idea that Panx1 does not contribute to gap junctional communication and thus does not form gap junction channels. Moreover, although our results suggest that decreased expression of Panx1 is accompanied by increased Cx43 expression, further studies are necessary to evaluate the extent to which such modulation occurs, especially in system were Panx1 is over-expressed.

In conclusion, the present study provides further evidence that phenomena attributed to Cx43 hemichannels or to the P2Z pore such as ATP release and dye uptake are due to Panx1 channels. Moreover, here we indicate that Panx1 channels are exquisitely tuned to respond to changes in extracellular environment by releasing "gliotransmitter".

Acknowledgments

References

Anderson CM, Bergher JP, Swanson RA. ATP-induced ATP release from astrocytes. J Neurochem. 2004; 88(1):246–256. [PubMed: 14675168]

Bao L, Locovei S, Dahl G. Pannexin membrane channels are mechanosensitive conduits for ATP. FEBS letters. 2004; 572(1–3):65–68. [PubMed: 15304325]

Baranova A, Ivanov D, Petrash N, Pestova A, Skoblov M, Kelmanson I, Shagin D, Nazarenko S, Geraymovych E, Litvin O, et al. The mammalian pannexin family is homologous to the invertebrate innexin gap junction proteins. Genomics. 2004; 83(4):706–716. [PubMed: 15028292]

Bargiota P, Krenz A, Hormuzdi SG, Ridder DA, Herb A, Barakat W, Penuela S, von Engelhardt J, Monyer H, Schwaninger M. Pannexins in ischemia-induced neurodegeneration. Proc Natl Acad Sci U S A. 2011; 108(51):20772–20777. [PubMed: 22147915]

Bruzzone R, Barbe MT, Jakob NJ, Monyer H. Pharmacological properties of homomeric and heteromeric pannexin hemichannels expressed in *Xenopus* oocytes. J Neurochem. 2005; 92(5): 1033–1043. [PubMed: 15715654]

Bruzzone R, Hormuzdi SG, Barbe MT, Herb A, Monyer H. Pannexins, a family of gap junction proteins expressed in brain. Proc Natl Acad Sci U S A. 2003; 100(23):13644–13649. [PubMed: 14597722]

Clarke TC, Williams OJ, Martin PE, Evans WH. ATP release by cardiac myocytes in a simulated ischaemia model: inhibition by a connexin mimetic and enhancement by an antiarrhythmic peptide. Eur J Pharmacol. 2009; 605(1–3):9–14. [PubMed: 19101539]

Contreras JE, Saez JC, Bukauskas FF, Bennett MV. Gating and regulation of connexin 43 (Cx43) hemichannels. Proc Natl Acad Sci U S A. 2003; 100(20):11388–11393. [PubMed: 13130072]

Contreras JE, Sanchez HA, Eugenin EA, Speidel D, Theis M, Willecke K, Bukauskas FF, Bennett MV, Saez JC. Metabolic inhibition induces opening of unapposed connexin 43 gap junction hemichannels and reduces gap junctional communication in cortical astrocytes in culture. Proc Natl Acad Sci U S A. 2002; 99(1):495–500. [PubMed: 11756680]

Dahl G. Gap junction-mimetic peptides do work, but in unexpected ways. Cell commun adhes. 2007; 14(6):259–264. [PubMed: 18392993]

Dahl G, Locovei S. Pannexin: to gap or not to gap, is that a question? IUBMB Life. 2006; 58(7):409–419. [PubMed: 16801216]

Dahl G, Werner R, Levine E, Rabadan-Diehl C. Mutational analysis of gap junction formation. Biophys J. 1992; 62(1):172–180. discussion 180–172. [PubMed: 1376165]

De Pina-Benabou MH, Srinivas M, Spray DC, Scemes E. Calmodulin kinase pathway mediates the K$^+$-induced increase in Gap junctional communication between mouse spinal cord astrocytes. J Neurosci. 2001; 21(17):6635–6643. [PubMed: 11517253]

De Vuyst E, Decrock E, De Bock M, Yamasaki H, Naus CC, Evans WH, Leybaert L. Connexin hemichannels and gap junction channels are differentially influenced by lipopolysaccharide and basic fibroblast growth factor. Mol Biol Cell. 2007; 18(1):34–46. [PubMed: 17079735]

Dobrowolski R, Sasse P, Schrickel JW, Watkins M, Kim JS, Rackauskas M, Troatz C, Ghanem A, Tiemann K, Degen J, Bukauskas FF, Civitelli R, Lewalter T, Fleischmann BK, Willecke K. The conditional connexin43G138R mouse mutant represents a new model of hereditary oculodentodigital dysplasia in humans. Hum Mol Genet. 2008; 17:539–554. [PubMed: 18003637]

el-Fouly MH, Trosko JE, Chang CC. Scrape-loading and dye transfer. A rapid and simple technique to study gap junctional intercellular communication. Exp Cell Res. 1987; 168(2):422–430. [PubMed: 2433137]

Hamilton NB, Attwell D. Do astrocytes really exocytose neurotransmitters? Nature reviews Neuroscience. 2010; 11(4):227–238.

Iacobas DA, Iacobas S, Urban-Maldonado M, Scemes E, Spray DC. Similar transcriptomic alterations in Cx43 knockdown and knockout astrocytes. Cell Commun Adhes. 2008; 15(1):195–206. [PubMed: 18649190]

Iglesias R, Dahl G, Qiu F, Spray DC, Scemes E. Pannexin 1: the molecular substrate of astrocyte "hemichannels". J Neurosci. 2009a; 29(21):7092–7097. [PubMed: 19474335]

Iglesias R, Locovei S, Roque A, Alberto AP, Dahl G, Spray DC, Scemes E. $P2X_7$ receptor-Pannexin1 complex: pharmacology and signaling. Am J Physiol Cell Physiol. 2008; 295(3):C752–760. [PubMed: 18596211]

Iglesias R, Spray DC, Scemes E. Mefloquine blockade of Pannexin1 currents: resolution of a conflict. Cell Commun Adhes. 2009b; 16(5–6):131–137. [PubMed: 20218915]

John GR, Scemes E, Suadicani SO, Liu JS, Charles PC, Lee SC, Spray DC, Brosnan CF. IL-1beta differentially regulates calcium wave propagation between primary human fetal astrocytes via pathways involving P2 receptors and gap junction channels. Proc Natl Acad Sci U S A. 1999; 96(20):11613–11618. [PubMed: 10500225]

Kang J, Kang N, Lovatt D, Torres A, Zhao Z, Lin J, Nedergaard M. Connexin 43 hemichannels are permeable to ATP. J Neurosci. 2008; 28(18):4702–4711. [PubMed: 18448647]

Lai CP, Bechberger JF, Thompson RJ, MacVicar BA, Bruzzone R, Naus CC. Tumor-suppressive effects of pannexin 1 in C6 glioma cells. Cancer Res. 2007; 67(4):1545–1554. [PubMed: 17308093]

Leybaert L, Braet K, Vandamme W, Cabooter L, Martin PE, Evans WH. Connexin channels, connexin mimetic peptides and ATP release. Cell Commun Adhes. 2003; 10(4–6):251–257. [PubMed: 14681025]

Locovei S, Bao L, Dahl G. Pannexin 1 in erythrocytes: function without a gap. Proc Natl Acad Sci U S A. 2006a; 103(20):7655–7659. [PubMed: 16682648]

Locovei S, Scemes E, Qiu F, Spray DC, Dahl G. Pannexin1 is part of the pore forming unit of the $P2X_7$ receptor death complex. FEBS letters. 2007; 581(3):483–488. [PubMed: 17240370]

Locovei S, Wang J, Dahl G. Activation of pannexin 1 channels by ATP through P2Y receptors and by cytoplasmic calcium. FEBS letters. 2006b; 580(1):239–244. [PubMed: 16364313]

Marques-da-Silva C, Chaves MM, Rodrigues JC, Corte-Real S, Coutinho-Silva R, Persechini PM. Differential modulation of ATP-induced $P2X_7$-associated permeabilities to cations and anions of macrophages by infection with Leishmania amazonensis. PLoS One. 2011; 6(9):e25356. [PubMed: 21966508]

Panchin Y, Kelmanson I, Matz M, Lukyanov K, Usman N, Lukyanov S. A ubiquitous family of putative gap junction molecules. Curr Biol. 2000; 10(13):R473–474. [PubMed: 10898987]

Panchin YV. Evolution of gap junction proteins - the pannexin alternative. J Exp Biol. 2005; 208(Pt 8):1415–1419. [PubMed: 15802665]

Parpura V, Scemes E, Spray DC. Mechanisms of glutamate release from astrocytes: gap junction "hemichannels", purinergic receptors and exocytotic release. Neurochem Internat. 2004; 45(2–3):259–264.

Pelegrin P, Surprenant A. Pannexin-1 mediates large pore formation and interleukin-1beta release by the ATP-gated $P2X_7$ receptor. The EMBO J. 2006; 25(21):5071–5082.

Pelegrin P, Surprenant A. Pannexin-1 couples to maitotoxin- and nigericin-induced interleukin-1beta release through a dye uptake-independent pathway. J Biol Chem. 2007; 282(4):2386–2394. [PubMed: 17121814]

Pelegrin P, Surprenant A. The $P2X_7$ receptor-pannexin connection to dye uptake and IL-1beta release. Purinergic Signal. 2009; 5(2):129–137. [PubMed: 19212823]

Qiu F, Wang J, Spray DC, Scemes E, Dahl G. Two non-vesicular ATP release pathways in the mouse erythrocyte membrane. FEBS Lett. 2011; 585(21):3430–3435. [PubMed: 21983290]

Qu Y, Misaghi S, Newton K, Gilmour LL, Louie S, Cupp JE, Dubyak GR, Hackos D, Dixit VM. Pannexin-1 is required for ATP release during apoptosis but not for inflammasome activation. J Immunol. 2011; 186(11):6553–6561. [PubMed: 21508259]

Retamal MA, Froger N, Palacios-Prado N, Ezan P, Saez PJ, Saez JC, Giaume C. Cx43 hemichannels and gap junction channels in astrocytes are regulated oppositely by proinflammatory cytokines released from activated microglia. J Neurosci. 2007; 27(50):13781–13792. [PubMed: 18077690]

Santiago MF, Veliskova J, Patel NK, Lutz SE, Caille D, Charollais A, Meda P, Scemes E. Targeting pannexin1 improves seizure outcome. PLoS One. 2011; 6(9):e25178. [PubMed: 21949881]

Scemes E. Nature of plasmalemmal functional "hemichannels". Biochim Biophys Acta. 2011 In press.

Scemes E, Giaume C. Astrocyte calcium waves: what they are and what they do. Glia. 2006; 54(7): 716–725. [PubMed: 17006900]

Scemes E, Suadicani SO, Dahl G, Spray DC. Connexin and pannexin mediated cell-cell communication. Neuron Glia Biol. 2007; 3(3):199–208. [PubMed: 18634611]

Scemes E, Suadicani SO, Spray DC. Intercellular communication in spinal cord astrocytes: fine tuning between gap junctions and P2 nucleotide receptors in calcium wave propagation. J Neurosci. 2000; 20(4):1435–1445. [PubMed: 10662834]

Schachter J, Motta AP, de Souza Zamorano A, da Silva-Souza HA, Guimaraes MZ, Persechini PM. ATP-induced $P2X_7$-associated uptake of large molecules involves distinct mechanisms for cations and anions in macrophages. J Cell Sci. 2008; 121(Pt 19):3261–3270. [PubMed: 18782864]

Seminario-Vidal L, Okada SF, Sesma JI, Kreda SM, van Heusden CA, Zhu Y, Jones LC, O'Neal WK, Penuela S, Laird DW, et al. Rho signaling regulates pannexin 1 - mediated ATP release from airway epithelia. J Biol Chem. 2011; 286(30):26277–26286. [PubMed: 21606493]

Silverman WR, de Rivero Vaccari JP, Locovei S, Qiu F, Carlsson SK, Scemes E, Keane RW, Dahl G. The pannexin 1 channel activates the inflammasome in neurons and astrocytes. J Biol Chem. 2009; 284(27):18143–18151. [PubMed: 19416975]

Sosinsky GE, Boassa D, Dermietzel R, Duffy HS, Laird DW, MacVicar B, Naus CC, Penuela S, Scemes E, Spray DC, et al. Pannexin channels are not gap junction hemichannels. Channels (Austin). 2011; 5(3):193–197. [PubMed: 21532340]

Suadicani SO, Brosnan CF, Scemes E. $P2X_7$ receptors mediate ATP release and amplification of astrocytic intercellular Ca^{2+} signaling. J Neurosci. 2006; 26(5):1378–1385. [PubMed: 16452661]

Suadicani SO, De Pina-Benabou MH, Urban-Maldonado M, Spray DC, Scemes E. Acute downregulation of Cx43 alters P2Y receptor expression levels in mouse spinal cord astrocytes. Glia. 2003; 42(2):160–171. [PubMed: 12655600]

Suadicani SO, Iglesias R, Spray DC, Scemes E. Point mutation in the mouse $P2X_7$ receptor affects intercellular calcium waves in astrocytes. ASN Neuro. 2009; 1(1) pii: e00005.

Thi MM, Urban-Maldonado M, Spray DC, Suadicani SO. Characterization of hTERT-immortalized osteoblast cell lines generated from wild-type and connexin43-null mouse calvaria. American journal of physiology Cell Physiol. 2010; 299(5):C994–C1006.

Torres A, Wang F, Xu Q, Fujita T, Dobrowolski R, Willecke K, Takano T, Nedergaard M. Extracellular Ca^{2+} acts as a mediator of communication from neurons to glia. Sci Signal. 2012; 5(208):ra8. [PubMed: 22275221]

Ye ZC, Wyeth MS, Baltan-Tekkok S, Ransom BR. Functional hemichannels in astrocytes: a novel mechanism of glutamate release. J Neurosci. 2003; 23(9):3588–3596. [PubMed: 12736329]
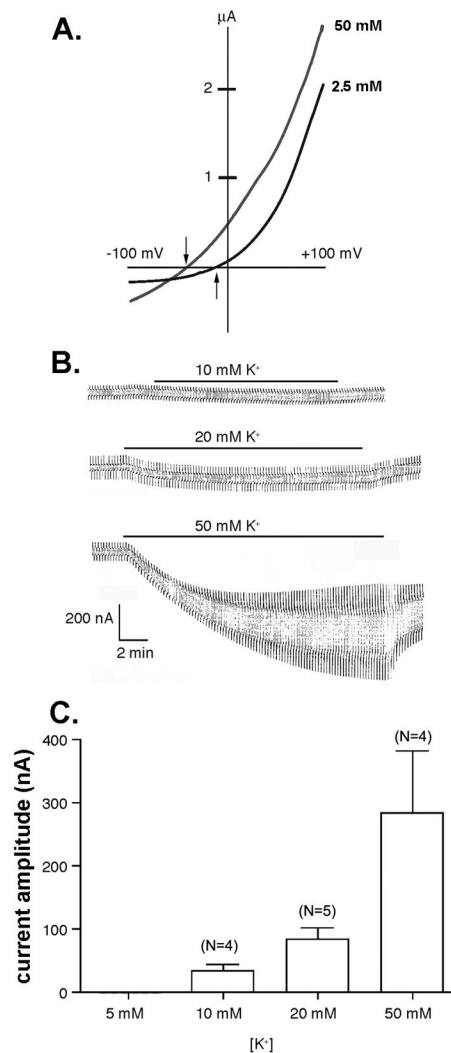
Figure 1. Elevated extracellular K$^+$ activates Panx1 channels in oocytes
(**A**) Example of currents recorded from mPanx1 expressing oocytes bathed in 2.5 and 50 mM K$^+$ solution and subjected to voltage ramps (−100 to +100 mV). Arrows indicate the activation voltage of Panx1 currents in these two conditions. (**B**) Whole cell recordings of mPanx1 oocytes bathed in 10, 20, and 50 mM K$^+$ obtained by applying +10 mV voltage steps (from a holding potential of −60 mV). (**C**) Mean ± s.e.m. values of current amplitudes obtained from experiments shown in part **B**; N as indicated in figure.
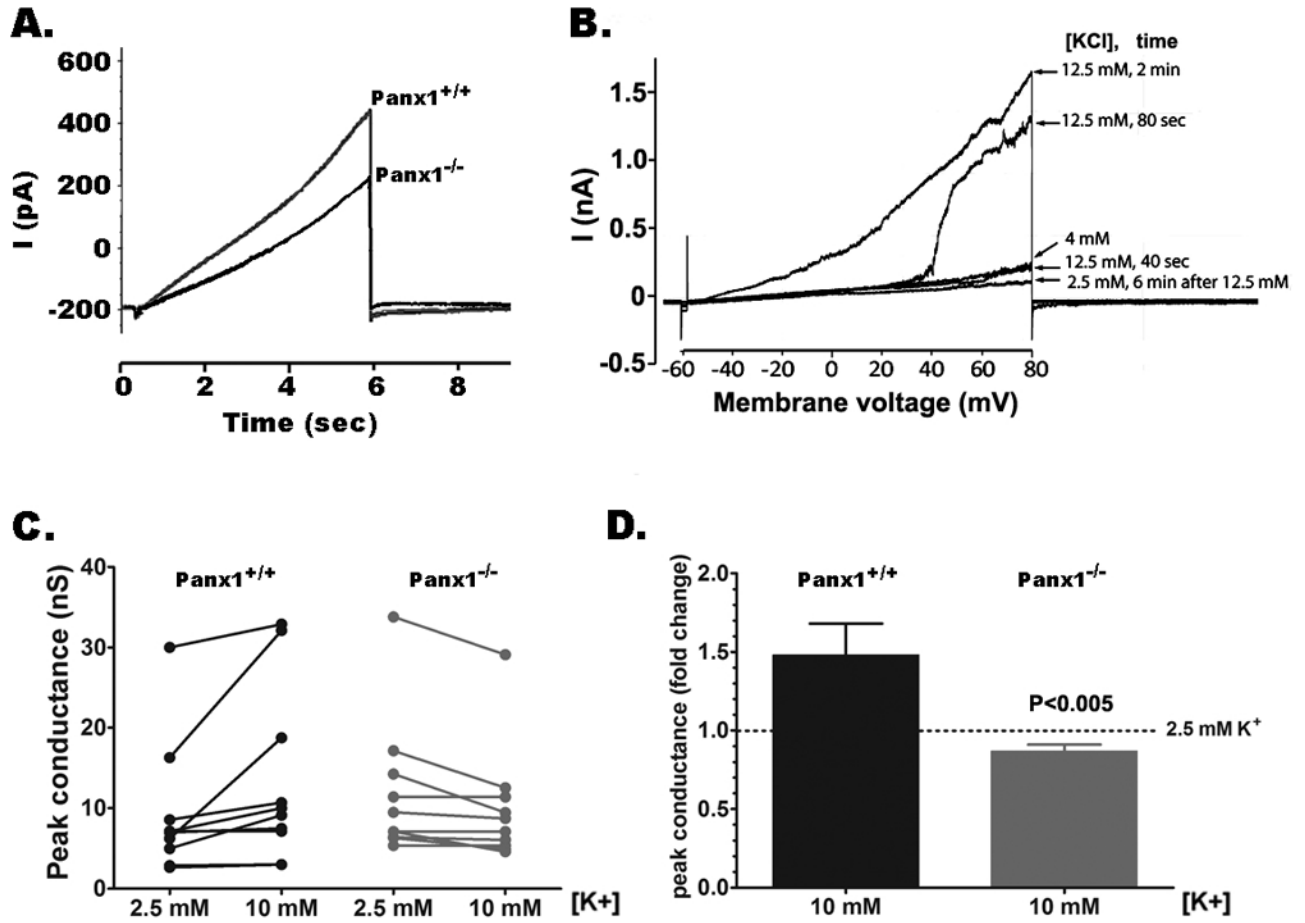
Figure 2. K⁺ sensitivity of astrocyte Panx1 currents
(**A**) Examples of whole cell recordings performed in solitary astrocytes derived from
Panx1$^{+/+}$ and Panx1$^{-/-}$ mice exposed to 5 mM K⁺ solution and subjected to voltage ramps
(−60mV to +80 mV, at 28 mV/sec; holding potential of −60mV). (**B**) Panx1 currents
recorded from Panx1$^{+/+}$ solitary are shown to be activated at negative membrane potentials
in a time dependent manner by increasing extracellular K⁺ concentrations from 4 to 12.5
mM. Six minutes after washout of 12.5 mM K⁺ solution with a 2.5 mM K⁺ solution, Panx1
currents were of smaller amplitudes than those recorded in 4 mM K⁺ solution (**C**) Peak
conductance of Panx1 channels recorded from 10 Panx1$^{+/+}$ and 11 Panx1$^{-/-}$ astrocytes
bathed in 2.5 and 10 mM K⁺ solutions. (**D**) Bar histograms of the mean ± s.e.m. values of
the fold changes in Panx1 peak conductance recorded from Panx1$^{+/+}$ and Panx1$^{-/-}$
astrocytes induced by 10 mM K⁺ solution normalized to those recorded at 2.5 mM K⁺
(dotted line).
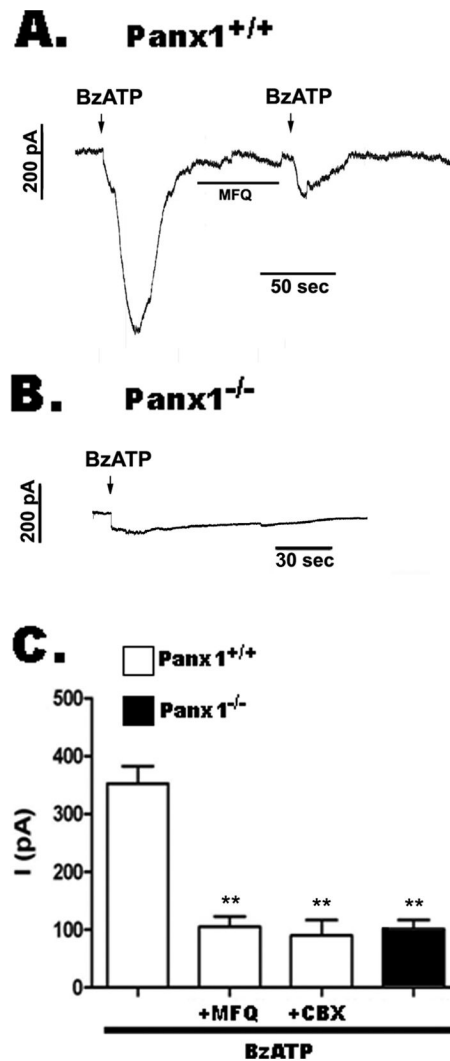
Figure 3. Panx1 channels contribute to P2X$_7$ receptor currents

(**A, B**) Examples of BzATP-induced whole cell currents recorded from (**A**) Panx1$^{+/+}$ and (**B**) Panx1$^{-/-}$ solitary astrocytes (holding potential of −60 mV). (**C**) Bar histograms of the mean ± s.e.m values of BzATP-induced currents recorded from solitary Panx1$^{+/+}$ astrocytes in the absence and presence of MFQ (100 nM) and CBX (50 µM). Note that BzATP current amplitudes recorded from Panx1$^{-/-}$ astrocytes are quite similar to those recorded from Panx1$^{+/+}$ in the presence of Panx1 channel blockers. **P<0.01 calculated from 4–6 independent recordings.
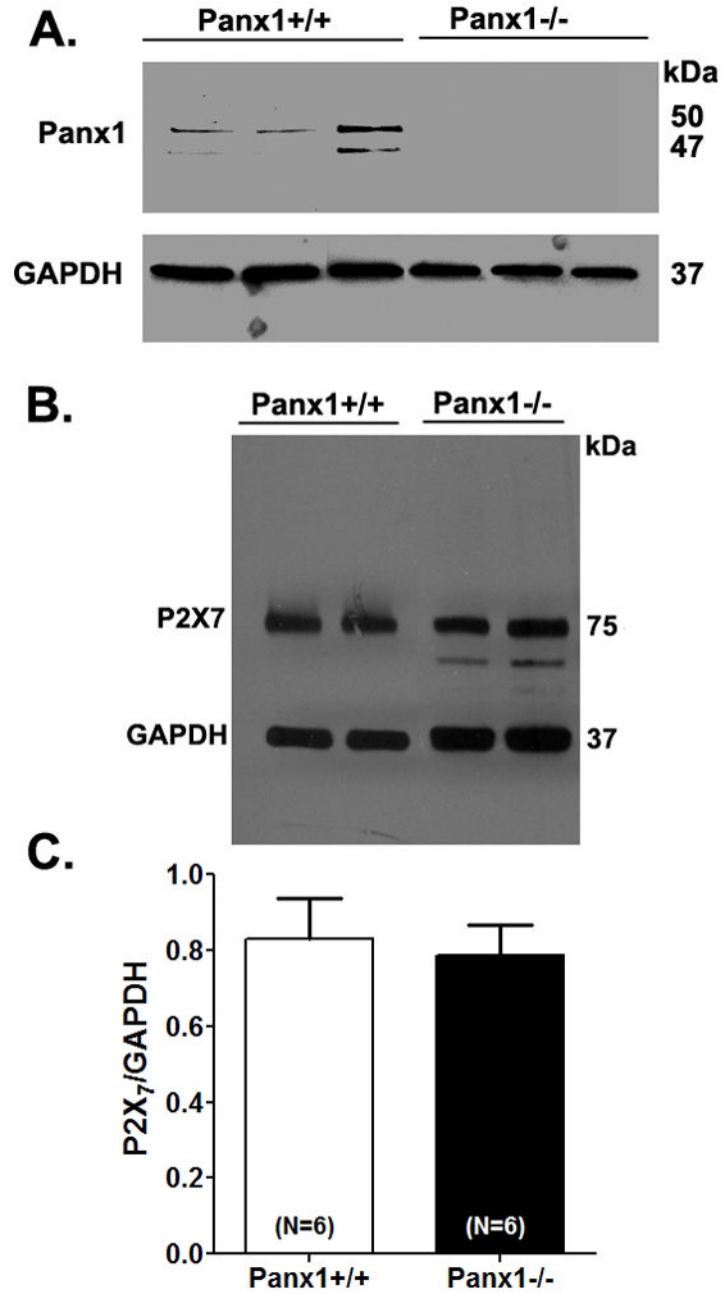
Figure 4. P2X$_7$ receptor expression is not altered in Panx1$^{-/-}$ cultured astrocytes
Representative western blots of (**A**) Panx1 and (**B**) P2X$_7$ receptor expression obtained from Panx1$^{+/+}$ and Panx1$^{-/-}$ cultured astrocytes. (**C**) Bar histogram of the mean ± s.e.m. values of P2X$_7$ expression levels (normalized to GAPDH) measured from 6 independent cultures of Panx1$^{+/+}$ and of Panx1$^{-/-}$ astrocytes.
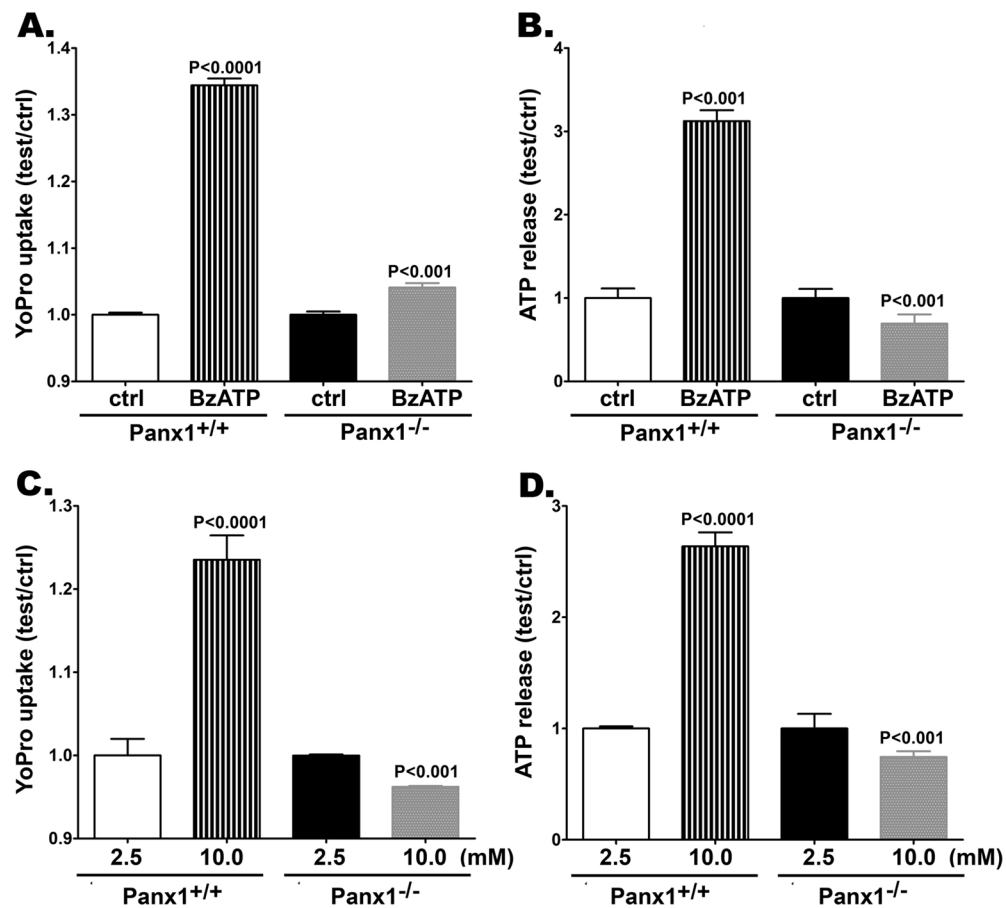
Figure 5. Panx1 channels mediate dye uptake and ATP release from cultured astrocytes
Bar histogram of the mean ± s.e.m. values of (**A**, **C**) Yopro-1 fluorescence changes relative to control conditions (ctrl) and (**B**, **D**) of ATP release from cultured Panx1$^{+/+}$ and Panx1$^{-/-}$ astrocytes induced by (**A**, **B**) a P2X$_7$ receptor agonist (300 μM BzATP) and (**C**, **D**) by 10 mM K$^+$ solution. P values were obtained using ANOVA analysis of variance followed by Tukey's multiple comparison tests. Data are from 3–8 independent experiments.
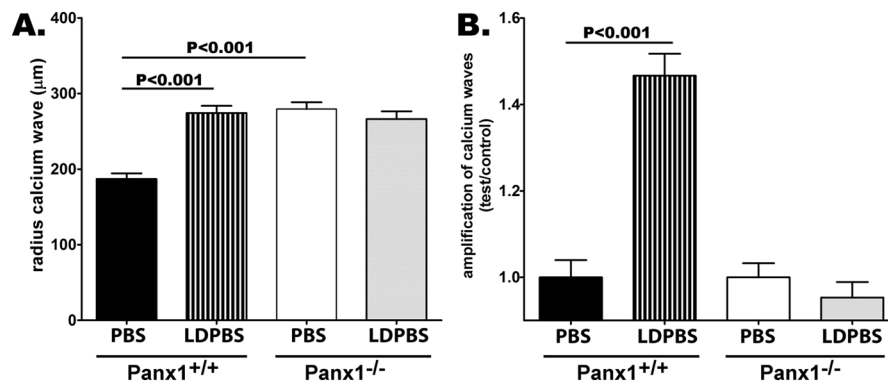
Figure 6. Impaired calcium wave amplification in cultured Panx1$^{-/-}$ astrocytes
(**A**) Bar histogram of the mean ± s.e.m. values of the radius of calcium wave spread between confluent cultures of Panx1$^{+/+}$ and Panx1$^{-/-}$ astrocytes bathed in divalent containing phosphate buffered solution (PBS) and in low divalent (LDPBS) solutions. Part (**B**) shows the amplification of calcium waves measured as the fold changes in radius of calcium wave spread recorded in Panx1$^{+/+}$ and Panx1$^{-/-}$ astrocytes exposed to LDPBS normalized to that obtained from the same cells bathed in PBS. P values were obtained by ANOVA analysis of variance followed by Tukey's multiple comparison tests. Values were obtained from 30–50 independent experiments performed on at least three different litters of each genotype.
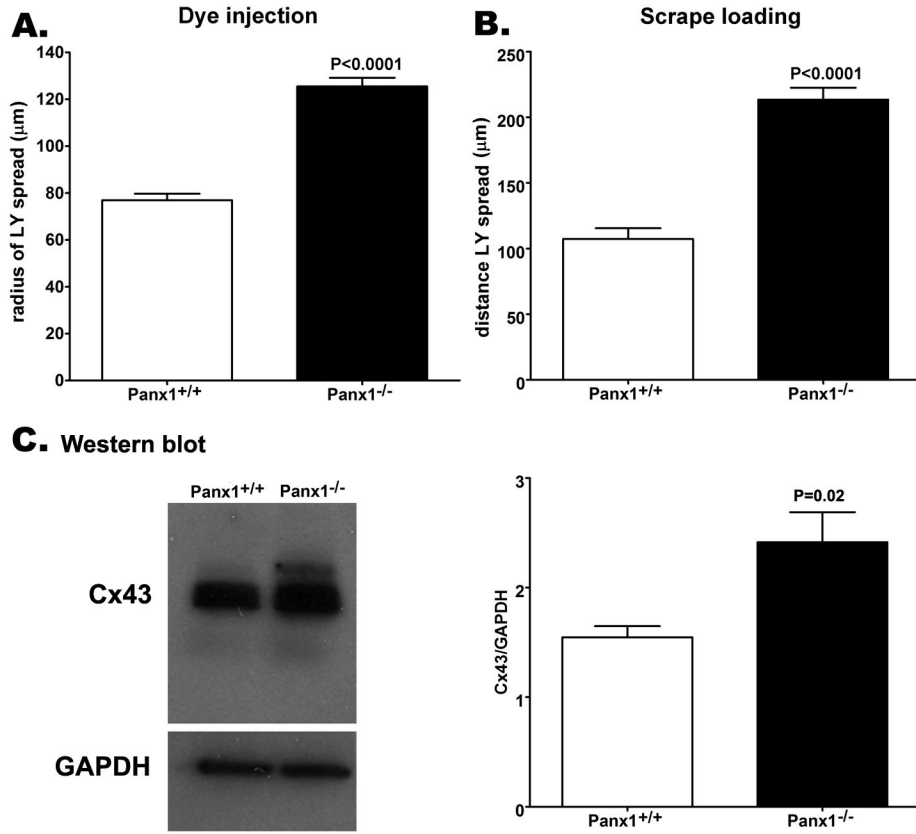
Figure 7. Increased Cx43 mediated coupling in Panx1$^{-/-}$ cultured astrocytes

Bar histograms of the mean ± s.e.m. values of the distance of dye spread (in μm) between Panx1$^{+/+}$ and Panx1$^{-/-}$ cultured astrocytes measured by (**A**) the LY microinjection and (**B**) the scrape loading techniques. (**C**) Representative western blot and analysis of Cx43 expression level changes in cultured astrocytes derived from 3 Panx1$^{+/+}$ and 3 Panx1$^{-/-}$ mice. Note the significant increase in Cx43 expression in relation to GAPDH in the Panx1$^{-/-}$ compared to Panx1$^{+/+}$ cells. P values were obtained by unpaired t-test.